

RESEARCH ARTICLE | SEPTEMBER 22 2015

Toward *ab initio* molecular dynamics modeling for sum-frequency generation spectra; an efficient algorithm based on surface-specific velocity-velocity correlation function

Tatsuhiko Ohto; Kota Usui; Taisuke Hasegawa; Mischa Bonn; Yuki Nagata



J. Chem. Phys. 143, 124702 (2015)

<https://doi.org/10.1063/1.4931106>



Articles You May Be Interested In

Vibrational spectroscopy of hydroxylated α -Al₂O₃(0001) surfaces with and without water: An *ab initio* molecular dynamics study

J. Chem. Phys. (July 2018)

Revealing the molecular structures of α -Al₂O₃(0001)-water interface by machine learning based computational vibrational spectroscopy

J. Chem. Phys. (September 2024)

Molecular dynamics study of two-dimensional sum frequency generation spectra at vapor/water interface

J. Chem. Phys. (March 2015)



Unlock the Full Spectrum.
From DC to 8.5 GHz.

Your Application. Measured.

[Find out more](#)



Toward *ab initio* molecular dynamics modeling for sum-frequency generation spectra; an efficient algorithm based on surface-specific velocity-velocity correlation function

Tatsuhiko Ohto,^{1,a)} Kota Usui,² Taisuke Hasegawa,³ Mischa Bonn,² and Yuki Nagata^{2,a)}

¹Graduate School of Engineering Science, Osaka University, 1-3 Machikaneyama, Toyonaka, Osaka 560-8531, Japan

²Max-Planck Institute for Polymer Research, Ackermannweg 10, 55128 Mainz, Germany

³Department of Chemistry, Graduate School of Science, Kyoto University, Sakyo-ku, Kyoto 606-8502, Japan

(Received 14 June 2015; accepted 3 September 2015; published online 22 September 2015)

Interfacial water structures have been studied intensively by probing the O–H stretch mode of water molecules using sum-frequency generation (SFG) spectroscopy. This surface-specific technique is finding increasingly widespread use, and accordingly, computational approaches to calculate SFG spectra using molecular dynamics (MD) trajectories of interfacial water molecules have been developed and employed to correlate specific spectral signatures with distinct interfacial water structures. Such simulations typically require relatively long (several nanoseconds) MD trajectories to allow reliable calculation of the SFG response functions through the dipole moment-polarizability time correlation function. These long trajectories limit the use of computationally expensive MD techniques such as *ab initio* MD and centroid MD simulations. Here, we present an efficient algorithm determining the SFG response from the surface-specific velocity-velocity correlation function (ssVVCF). This ssVVCF formalism allows us to calculate SFG spectra using a MD trajectory of only \sim 100 ps, resulting in the substantial reduction of the computational costs, by almost an order of magnitude. We demonstrate that the O–H stretch SFG spectra at the water-air interface calculated by using the ssVVCF formalism well reproduce those calculated by using the dipole moment-polarizability time correlation function. Furthermore, we applied this ssVVCF technique for computing the SFG spectra from the *ab initio* MD trajectories with various density functionals. We report that the SFG responses computed from both *ab initio* MD simulations and MD simulations with an *ab initio* based force field model do not show a positive feature in its imaginary component at 3100 cm^{-1} . © 2015 AIP Publishing LLC. [<http://dx.doi.org/10.1063/1.4931106>]

I. INTRODUCTION

At surfaces and interfaces, the composition and arrangement of molecules are often different from those in the bulk, and both determine, and are determined by, how the material interacts with its surroundings. Molecular processes at interfaces play a key role in disciplines as diverse as electrochemistry, environmental science, biophysics, and catalysis. As such, knowledge of specifically the interfacial composition and ordering of molecules is essential for a wide range of fields.

Sum-frequency generation (SFG) is a second-order nonlinear process and has been used to characterize molecules at interfaces through their vibrational responses. Thanks to the selection rule of SFG spectroscopy, the resonant SFG response vanishes in centro-symmetric media, allowing us to probe response of specifically the interfacial molecules with a net orientation at the interface.¹ This technique has been successfully applied to various systems including polymer-water,² liquid-liquid,^{3–5} protein-water,^{6–9} water-air,^{10–26} water-solid,^{27–30} and water-lipid^{31–34} interfaces. A distinct advantage

of vibrational SFG spectroscopy over other surface-specific techniques is that SFG can operate under ambient conditions and can access to the microscopic structure of liquid interfaces where the molecules are highly mobile.

Among various liquid interfaces, the aqueous interfaces have been intensively studied, because they bear relevance to atmospheric chemistry, electrochemistry, and biology; the rates for the evaporation and condensation of water at water-air interface affects the aerosol nucleation and cloud formation,^{35–37} while the water-solid interfaces play a central role in various catalytic reactions such as the photo-catalytic reactions occurring at the water-TiO₂ interface.³⁸ Experimental SFG studies over the past two decades have successfully unveiled the structure of the aqueous interfaces; the presence of the dangling O–H and hydrogen-bonded O–H groups at the water-air interface is evident from the sharp SFG peak centered at 3700 cm^{-1} and the broad band covering the frequency range $3200\text{--}3400\text{ cm}^{-1}$, respectively.¹ The delicate balance between these dangling O–H and hydrogen-bonded O–H groups has been examined by using the isotopically diluted water; the isotope H/D change gives rise to the different zero point energy, resulting in the enrichment of the dangling O–H groups relative to dangling O–D groups at the air interface of H₂O/D₂O mixtures.^{19,20} Further SFG studies at the

^{a)}Authors to whom correspondence should be addressed. Electronic addresses: ohto@molecules.jp and nagata@mpip-mainz.mpg.de

water-air interface using heterodyne-detection of the signal have allowed us to independently determine the real and imaginary part of the interfacial SFG response. The imaginary component is the surface equivalent of the bulk IR absorption spectrum, and its sign denotes the orientation of the O–H groups relative to the surface normal. These studies have revealed positive (upwards-oriented) 3100 cm^{-1} and negative (downwards-oriented) 3400 cm^{-1} SFG features are present, in addition to the positive 3700 cm^{-1} peak.^{21,23,33}

Motivated by these experimental SFG studies, several approaches to simulate the SFG spectra have been developed,^{39–48} enabling us to compare the simulated spectra directly with the experimentally measured data. In particular, all-atom molecular dynamics (MD) simulations have been used to sample the molecular configurations and/or calculate the second-order susceptibility of liquid surface. Among the various liquid interfaces, one of the simplest aqueous interfaces for MD simulations is the water-air interface, since the structure and dynamics at the water-air interface are governed solely by water-water interactions. The 3700 cm^{-1} peak has been successfully reproduced with the known water models such as SPC/E water model,⁴⁹ while the positive $\sim 3100\text{ cm}^{-1}$ SFG band that had been reported in experiments could not be reproduced in a straightforward way. The first simulation for reproducing the 3100 cm^{-1} band has been reported by Ishiyama and Morita, where they improved the optical response calculation and attributed the molecular origin of the 3100 cm^{-1} band to the induced dipole moment through the anisotropic component of the polarizability.^{53–55} On the other hand, Skinner and co-workers have developed a novel force field model including the three-body effects,⁵² with which this 3100 cm^{-1} positive band is also reproduced.^{50–52} These different force field models give rise to the distinct physical pictures of the water-air interface; Morita and co-workers have insisted that SFG spectra are relatively insensitive to the details of the interfacial water structure,^{53–55} whereas Skinner and co-workers have claimed that the structure is strongly modulated by the three-body effect at the interface in contrast to in the bulk.^{50,51} Apparently, the different force field models provide contradictory interpretations of the SFG spectra.

In contrast to the approaches using force field models which depend strongly on the functions used in the force field modeling and the fitting procedure, *ab initio* MD (AIMD) simulations offer a more unambiguous approach, since the molecular forces are calculated from the electronic structure theory.^{59–70} The AIMD simulations reported here include the charge redistribution at interfaces intrinsically, and therefore have the potential to provide a picture for the structure of the water-air interface with minimal assumptions. The first AIMD simulation for computing the SFG spectrum at the water-air interface has been reported by Sulpizi *et al.*⁶⁵ However, in spite of the apparent advantages of AIMD simulation and its frequent use at interfaces,^{71–73} so far no other AIMD simulation for calculating the SFG spectra has been reported. This is presumably because AIMD simulation is computationally quite demanding to calculate the SFG spectra; a few nanosecond MD trajectory would be required to calculate the spectra when the dipole moment-polarizability (μ - α) time-correlation functions are Fourier transformed.^{42,53} Indeed, the

reported AIMD-based SFG spectrum was computed with a few tens of picoseconds AIMD trajectory, and was correspondingly noisy, presumably because of the insufficient convergence of the time-correlation function.⁶⁵ Since the resulting contribution from the bulk region should be much smaller than the contribution from the interfacial region, the simulation of the SFG spectra is computationally much more expensive than that of the IR spectra. Furthermore, we need to apply the external electric field to calculate the molecular polarizability,⁶⁵ which requires additional computational cost. As such, completing AIMD simulations for calculating the SFG spectra via the μ - α time-correlation functions are at present not practically feasible. To overcome these drawbacks, an efficient algorithm to calculate SFG spectra with a relatively short MD trajectory (up to $\sim 100\text{ ps}$) is urgently required to enable the AIMD or centroid⁷⁴ AIMD modeling of the O–H stretch SFG spectra.

Furthermore, AIMD simulation for calculating SFG spectra is essential to model the water-solid interfaces, where the use of the force field model is limited due to the improper description of the induced surface charges with the non-polarizable force field model. This may be overcome by using the polarizable force field models, but to do so, we need to construct the polarizable force field model by performing *ab initio* calculations for several molecular conformations and mapping the information onto the force field model.^{75,76} Since AIMD simulation can include the charge redistribution at interfaces intrinsically, it would be preferred for computing the spectra at the water-solid interfaces.^{72,77–79}

Here, we present an efficient algorithm to simulate SFG spectra of the water's O–H stretch mode with a few tens of picoseconds AIMD trajectory, which employs the velocity-velocity correlation function (VVCF). Since atom velocities arise solely from the nuclear motions and are insensitive to fluctuations of the electronic structures, the convergence of the VVCF would require much shorter MD trajectories compared with the dipole-dipole or polarizability-polarizability time correlation functions, accelerating the computation of vibrational spectra. We derive the formula for the surface-specific VVCF (ssVVCF) corresponding to the SFG response function. The ssVVCF differs from the VVCF in that the ssVVCF gives zero in a centrosymmetric medium, ensuring that the ssVVCF probes only the surface-specific molecular responses. The ssVVCF formalism is very suitable for the AIMD simulation, not only because the convergence of the time correlation function can be achieved with shorter MD trajectories but also because the computation of the molecular polarizability can be skipped.

In addition to ready access to the correlation function for individual O–H groups, this computation algorithm can also truncate the cross-correlation terms of the ssVVCF which represent the coupling of different O–H stretch chromophores, in the same manner as the truncated function formalism for the μ - α time correlation function.^{42,80} By controlling the truncation cutoff distance of the ssVVCF, we can examine the effects of the inter/intra-molecular couplings on the SFG spectra. The SFG spectrum calculated without the cross-correlation terms, termed surface-specific velocity-velocity autocorrelation function (ssVVAF), corresponds to the O–H stretch

response of an isolated HDO molecule in the isotopically diluted water. The presented ssVVCF algorithm, therefore, would be a promising approach to examine the surface-specific vibrational responses at aqueous interfaces.

The organization of this paper is as follows. In Sec. II, we derive the ssVVAF/ssVVCF formalisms corresponding to the SFG response function. In Sec. III, the force field MD and AIMD simulation protocols are given. In Sec. IV, we compare the simulated SFG spectra via the ssVVAF/ssVVCF formalisms with the spectra calculated from the $\mu\text{-}\alpha$ time correlation function at the water-air interface. The MD trajectory required for achieving convergence of the SFG response will be discussed. Furthermore, we show the SFG spectra at the water-air interface simulated with the AIMD trajectories with various density functionals. Conclusions are given in Sec. V.

II. EFFICIENT ALGORITHM FOR CALCULATING SFG SPECTRA

A. IR response function via VVAF

First, we review the formulation of the IR response function based on the VVAF. From the fluctuation-dissipation theorem, the first-order IR response function can be related to the dipole-dipole correlation function as⁸¹

$$\begin{aligned} \chi_{ab}^{(1)}(\omega) &= \frac{Q(\omega)}{\omega} \int_0^\infty dt e^{-i\omega t} \left\langle \sum_{i,j} \dot{\mu}_{b,j}(0) \mu_{a,i}(t) \right\rangle \\ &= \frac{Q(\omega)}{i\omega^2} \int_0^\infty dt e^{-i\omega t} \left\langle \sum_{i,j} \dot{\mu}_{b,j}(0) \dot{\mu}_{a,i}(t) \right\rangle, \end{aligned} \quad (1)$$

where $\mu_{a,i}(t)$ is the a component of the dipole moment for the i th molecule at time t . $Q(\omega)$ is the quantum correction factor.

The molecular dipole moment can be decomposed into the permanent and transition dipole moments,

$$\vec{\mu}_i(t) = B_i(t) \left(\vec{\mu}_i^0 + \sum_n \mu'_{i,n} \vec{q}_{i,n}(t) \right), \quad (2)$$

where $\vec{q}_{i,n}(t)$ denotes the normal mode vector n of molecule i at time t , $\vec{\mu}_i^0$ the permanent dipole moment for molecule i , and $\mu'_{i,n}$ the transition dipole moment for the normal mode n . $\vec{q}_{i,n}(t)$, $\vec{\mu}_i^0$, and $\mu'_{i,n}$ are defined in the molecular frame, and $B_i(t)$ is the rotational matrix converting from the local frame for molecule i to the lab-frame at time t .

Here, we focus on the water O–H stretch response. Since the dynamics of $B_i(t)\vec{\mu}_i^0$ are governed by the librational motions and the O–H stretch mode frequency is well-separated from the librational mode frequency, these motions can presumably be treated separately (see the Appendix). By

inserting Eq. (2) into (1), the IR response function can be recast as

$$\begin{aligned} \chi_{ab}^{(1)}(\omega) &= \frac{Q(\omega)}{i\omega^2} \int_0^\infty dt e^{-i\omega t} \\ &\times \left\langle \sum_{i,j} \sum_{m,n} \mu'_{j,m} \mu'_{i,n} \vec{q}_{b,j,m}^{\text{lab}}(0) \vec{q}_{a,i,n}^{\text{lab}}(t) \right\rangle, \end{aligned} \quad (3)$$

where $\vec{q}_{i,n}^{\text{lab}}(t) \equiv B_i(t) \vec{q}_{i,n}(t)$. Since the normal mode of the water O–H stretch is dominated by the variation of the intramolecular O–H bonds, $\vec{q}_{i,n}^{\text{lab}}(t)$ can be replaced by the i th O–H bond vector $\vec{r}_{i'}^{\text{OH}}(t)$.⁸² The IR signal is, thus, given by

$$\chi_{ab}^{(1)}(\omega) = \frac{Q(\omega) \mu_{\text{str}}^2}{i\omega^2} \int_0^\infty dt e^{-i\omega t} \left\langle \sum_{i',j'} \vec{r}_{b,j'}^{\text{OH}}(0) \vec{r}_{a,i'}^{\text{OH}}(t) \right\rangle, \quad (4)$$

where μ'_{str} is the transition dipole moment of the O–H stretch mode. This demonstrates that the IR response function is connected with the VVAF.

B. SFG response function via ssVVAF

We develop a formalism of the ssVVAF relevant to the SFG response functions. The abc component of the SFG response function can be calculated from the $\mu\text{-}\alpha$ time correlation function,

$$\begin{aligned} \chi_{abc}^{\text{res},(2)}(\omega) &= \frac{Q(\omega)}{\omega} \int_0^\infty dt e^{-i\omega t} \left\langle \sum_{i',j'} \dot{\mu}_{c,i}(0) \alpha_{ab,j}(t) \right\rangle \\ &= \frac{Q(\omega)}{i\omega^2} \int_0^\infty dt e^{-i\omega t} \left\langle \sum_{i',j'} \dot{\mu}_{c,i}(0) \dot{\alpha}_{ab,j}(t) \right\rangle, \end{aligned} \quad (5)$$

where $\alpha_{ab,j}(t)$ is the ab component of the polarizability for j th water molecule at time t . By decomposing the molecular polarizability tensor $\vec{\alpha}$ into the permanent and the transition polarizabilities,

$$\vec{\alpha}_i(t) = B_i^\dagger(t) \left(\vec{\alpha}_i^0 + \sum_n \vec{\alpha}'_{i,n} \vec{q}_{i,n}(t) \right) B_i(t). \quad (6)$$

$\vec{\alpha}$ can be parameterized by using two O–H bond polarizabilities, $\vec{\alpha}_1^{\text{OH}}$ and $\vec{\alpha}_2^{\text{OH}}$,⁴¹ as

$$\vec{\alpha}_i(t) = B_i^\dagger(t) \left(\vec{\alpha}_{i1}^{\text{OH}}(t) + \vec{\alpha}_{i2}^{\text{OH}}(t) \right) B_i(t). \quad (7)$$

Ab initio calculations show that the diagonal elements of the bond polarizability are dominated by the variation of the O–H distance, while the off-diagonal elements are negligibly small compared with the diagonal elements.⁴¹ Therefore, the bond polarizability can be expanded in terms of the O–H bond distance as

$$\vec{\alpha}_{i'}^{\text{OH}}(t) = \begin{pmatrix} \alpha_{xx}^0 + \frac{\partial \alpha_{xx}}{\partial r^{\text{OH}}} |r_{i'}^{\text{OH}}| & 0 & 0 \\ 0 & \alpha_{yy}^0 + \frac{\partial \alpha_{yy}}{\partial r^{\text{OH}}} |r_{i'}^{\text{OH}}| & 0 \\ 0 & 0 & \alpha_{zz}^0 + \frac{\partial \alpha_{zz}}{\partial r^{\text{OH}}} |r_{i'}^{\text{OH}}| \end{pmatrix}. \quad (8)$$

When $\alpha_{xx}^0 = \alpha_{yy}^0 = \alpha_{zz}^0 \equiv \alpha^0$ and $\frac{\partial \alpha_{xx}^0}{\partial r_{OH}} = \frac{\partial \alpha_{yy}^0}{\partial r_{OH}} = \frac{\partial \alpha_{zz}^0}{\partial r_{OH}} \equiv \alpha'_{str}$ are assumed, Eq. (7) reduces to $\dot{\alpha}_i(t) = \dot{\alpha}_{i1}^{OH}(t) + \dot{\alpha}_{i2}^{OH}(t)$. The SFG response function for the water O–H stretch can be written as

$$\chi_{abc}^{\text{res},(2)}(\omega) = \begin{cases} \frac{Q(\omega) \mu'_{str} \alpha'_{str}}{i\omega^2} \int_0^\infty dt e^{-i\omega t} \left\langle \sum_{i',j'} \dot{r}_{c,j'}^{OH}(0) \frac{\dot{r}_{j'}^{OH}(t) \cdot \vec{r}_{j'}^{OH}(t)}{|\dot{r}_{j'}^{OH}(t)|} \right\rangle & a = b \\ 0 & a \neq b \end{cases} . \quad (9)$$

Although this correlation function consists of the velocity of the atoms ($\dot{r}(t)$) similar to the VVAF of Eq. (4), this gives zero when $\langle r(t) \rangle = 0$, making Eq. (9) surface-specific. We term the correlation function in Eq. (9) as the ssVVAF. Note that the present formalisms using the relative velocities of the hydrogen and oxygen atoms were derived for the O–H stretch mode of water. To calculate the SFG spectra for other vibrational modes such as bending or librational modes, we need to define the relative velocities between atoms which represent the vibrational mode and construct the time-correlation function using these velocities. In other words, by properly choosing the relative velocities for the vibrational modes in interest, the SFG selection rules hold in the current formalisms.

C. Intra-/intermolecular coupling in ssVVCF

Above, we described the formalism to calculate the time autocorrelation function for individual O–H stretch chromophores. However, when the interactions are present between O–H stretch chromophores, the vibrational modes for these chromophores can be coupled, both inter- and intramolecularly, and the coupling will affect the vibrational spectra. Experimentally, this is confirmed by comparing IR/Raman/SFG spectra of neat H₂O and isotopically diluted H₂O.^{84,85}

To include these contributions in the simulated spectra, we need to calculate the cross-correlation terms beyond the auto-correlation function given in Eq. (9). The truncating response function formalism has been used to incorporate the cross-correlation with the response functions, by which the cross-correlation terms can be included in the response function with the tunable cutoff r_t for the geometrical distance of the chromophores. A ssVVAF can be directly extended to the ssVVCF and thus the SFG susceptibility is given by

$$\chi_{aac}^{\text{res},(2)}(\omega; r_t) = \frac{Q(\omega) \mu'_{str} \alpha'_{str}}{i\omega^2} \int_0^\infty dt e^{-i\omega t} \times \left\langle \sum_{i',j'} g_t(r_{ij}(0); r_t) \dot{r}_{c,j'}^{OH}(0) \frac{\dot{r}_{j'}^{OH}(t) \cdot \vec{r}_{j'}^{OH}(t)}{|\dot{r}_{j'}^{OH}(t)|} \right\rangle . \quad (10)$$

Here, $r_{ij}(t)$ is the distance between the center of masses of chromophores i and j at time t , and $g_t(r; r_t)$ is the function to control the cross-correlation terms with the cross-correlation cutoff of r_t and is given by

$$g_t(r; r_t) = \begin{cases} 1 & \text{for } r \leq r_t \\ 0 & \text{for } r > r_t \end{cases} . \quad (11)$$

D. Non-Condon effects

When deriving Eqs. (9) and (10), we assumed that the transition dipole moment and polarizability were frequency-independent (Condon approximation). However, since the strength of the hydrogen bond with the neighboring water molecules strongly affects the frequency of the O–H stretch mode as well as the amplitude of the vibrational transition dipole moment and polarizability of a water molecule in liquid water, this assumption is largely violated (non-Condon effects). In fact, the amplitude of the transition dipole moment for the 3200 cm⁻¹ O–H stretch mode is ~5 times larger than that at 3600 cm⁻¹.⁸⁶

These effects can be included in ssVVAF (Eq. (9)) and ssVVCF (Eq. (10)) by replacing the frequency independent transition dipole moment μ' (transition polarizability α') with the frequency-dependent transition dipole moment $\mu'(\omega)$ (frequency-dependent transition polarizability $\alpha'(\omega)$). Then, Eq. (11) can be recast as

$$\chi_{aac}^{\text{res},(2)}(\omega; r_t) = \frac{Q(\omega) \mu'(\omega) \alpha'(\omega)}{i\omega^2} \int_0^\infty dt e^{-i\omega t} \times \left\langle \sum_{i',j'} g_t(r_{ij}(0); r_t) \dot{r}_{c,j'}^{OH}(0) \frac{\dot{r}_{j'}^{OH}(t) \cdot \vec{r}_{j'}^{OH}(t)}{|\dot{r}_{j'}^{OH}(t)|} \right\rangle . \quad (12)$$

The transition dipole moment $\mu'(\omega)$ and polarizability $\alpha'(\omega)$ were parameterized by Skinner and co-workers, which gives^{86,87}

$$\begin{aligned} \mu'(\omega) &\equiv \left(1.377 + \frac{53.03(3737 - \omega)}{6932.2} \right) \mu^0, \\ \alpha'(\omega) &\equiv \left(1.271 + \frac{6.287(3737 - \omega)}{6932.2} \right) \alpha^0, \end{aligned} \quad (13)$$

where ω is in cm⁻¹. The solvent effects such as induced dipole moment and polarizability are implicitly included with Eq. (13).

III. SIMULATION PROTOCOLS

A. Force field MD simulation

We ran MD simulation at the water-air interface at 305 K. We used an *ab initio*-based polarizable force field model for water.^{80,88} For the MD simulation at the water-air interface, we prepared 32 different initial coordinates from which the MD simulations were run in the NVE ensemble. After 100 ps MD runs to ensure equilibration of the system at the water-air interface, we performed 300 ps MD runs where we recorded

the MD trajectories every 4 fs. The time step for integrating the equation of motion was set to 0.4 fs. The simulation cell was set to $26.6 \text{ \AA} \times 26.6 \text{ \AA} \times 160 \text{ \AA}$ with periodic boundary conditions, where 500 water molecules were contained. Simulation details can also be found in Ref. 113.

The force field used here overestimates the O–H stretch IR peak frequency of the bulk water by ~4% compared to the experimentally determined values.⁸⁸ Therefore, when calculating the SFG spectra, we scaled down the frequency by 4%. For the quantum correction factor in Eq. (1), we used the harmonic correction which is expressed by⁹⁰

$$Q(\omega) = \beta\hbar\omega/(1 - \exp(-\beta\hbar\omega)), \quad (14)$$

where $\beta = 1/kT$ is the inverse temperature. For the Fourier transformation of the time correlation function, we applied the Hann window function,

$$f(t) = \begin{cases} \cos^2(\pi t/2\tau) & \text{for } 0 < t < \tau \\ 0 & \text{for } t > \tau \end{cases}. \quad (15)$$

B. AIMD simulation

AIMD simulation of the water-air interface was performed at 320 K. We employed Becke-Lee-Yang-Parr (BLYP),^{91,92} Perdew-Burke-Ernzerhof (PBE),⁹³ and revised PBE (revPBE)⁹⁴ exchange-correlation functionals and the TZV2P basis sets. The core electrons were described by the Goedecker-Teter-Hutter pseudopotential⁹⁵ and the real-space density cutoff was set to 400 Ry.⁹⁶ The van der Waals interaction, which is important to reproduce the water density and dynamics,^{71,97,98} was included via the Grimme's D3 method.⁹⁹ Furthermore, to highlight the effects of the van der Waals correction on the SFG spectrum of water, we also performed AIMD simulation at the BLYP/TZV2P level of theory without the van der Waals corrections. The MD simulations were run in the NVT ensemble and the temperature was controlled by using the method of the canonical sample through velocity rescaling.⁸⁹ 80 ps MD runs were performed for computing the SFG spectra, after 20 ps MD runs for equilibrating the system. The time step for integrating the equation of motion was set to 0.4 fs. The $13.2 \text{ \AA} \times 13.2 \text{ \AA} \times 50 \text{ \AA}$ simulation cell with periodic boundary conditions contained 80 water molecules. The calculations were performed with the QUICKSTEP method¹⁰⁰ implemented in the CP2K code.¹⁰¹ For the SFG spectra calculation, we used the same harmonic correction factor (Eq. (14)) and the same Hann window function (Eq. (15)) in the same manner as the force field MD simulation, while the frequency axis was not scaled.

IV. RESULTS AND DISCUSSIONS

A. Accuracy of SFG spectrum based on ssVVCF formalism

To explore the reproducibility of the SFG response function based on the ssVVCF formalism, we simulated the O–H stretch SFG spectra at the water-air interface from the μ - α correlation function (Eq. (5)) as well as the ssVVCF (Eq. (12)) formalisms with a cutoff radius of $r_t = 2 \text{ \AA}$. Note that with

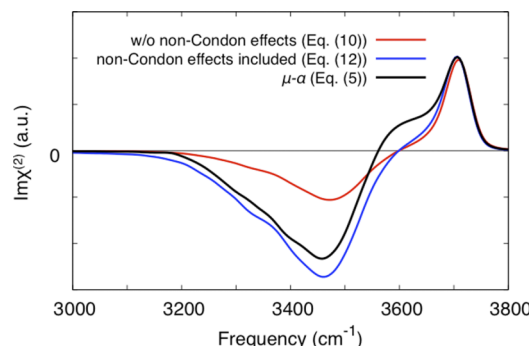


FIG. 1. Simulated O–H stretch SFG spectra without the non-Condon effect (Eq. (10)) and with the non-Condon effect (Eq. (12)) using a 6.4 ns MD trajectory. The SFG spectrum calculated via the μ - α correlation function using a 9.6 ns MD trajectory is also plotted. For these calculated spectra, a correlation cutoff of $r_t = 2 \text{ \AA}$ was used.

$r_t = 2 \text{ \AA}$, only the correlation of the neighboring O–H groups in a single water molecule is included. The simulated spectra are shown in Fig. 1. The SFG spectra simulated via the ssVVCF formalism are similar to that simulated via the μ - α time correlation function; not only the peak positions but also the peak intensities are in good agreement for the hydrogen bonded O–H (negative $\sim 3450 \text{ cm}^{-1}$) and free O–H (positive $\sim 3700 \text{ cm}^{-1}$) stretch peak. A major difference can be seen at $\sim 3600 \text{ cm}^{-1}$, where a shoulder is apparent in the μ - α spectrum. This shoulder originates from the anti-symmetric stretch mode of the interfacial water molecules with the two donor hydrogen bonds.²² This indicates that the coupling of these two O–H stretch modes in a single molecule may not be fully accounted for by the ssVVCF formalism. Nevertheless, the ssVVCF formalism reproduces the SFG spectra calculated via the μ - α time correlation function very accurately. The comparison of the SFG spectra with and without the non-Condon effects (Eqs. (12) and (10), respectively) indicates that the inclusion of the non-Condon effects is crucial to reproduce the SFG amplitude accurately. Finally, it should be noted that the SFG spectra simulated from the MD trajectory with the *ab initio*-based force field model⁸⁸ do not show a positive 3100 cm^{-1} feature.²¹

B. Effects of intermolecular couplings

We subsequently investigated the effect of intermolecular coupling by simulating the O–H stretch SFG spectra with $r_t = 2, 3, 4, 5$, and 6 \AA (see Fig. 2). For both formulas, the cross-correlation term dramatically enhanced the negative $\sim 3300 \text{ cm}^{-1}$ feature and reduced the negative $\sim 3450 \text{ cm}^{-1}$ feature through the intermolecular coupling. This trend can be equally seen in the IR spectra in liquid water.⁸⁶

C. Efficiency of SFG spectrum calculation with ssVVCF

Above, we have shown that the SFG spectrum calculated from the ssVVCF formalism accurately reproduces the spectrum calculated from the μ - α time correlation function. To demonstrate that the ssVVCF formalism is a computationally inexpensive algorithm compared with the μ - α time correlation

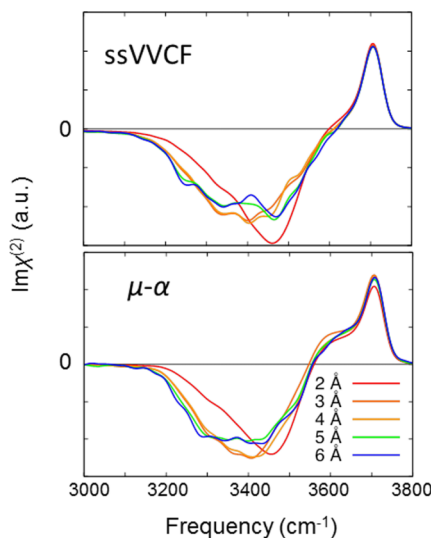


FIG. 2. Simulated O–H stretch SFG spectra using the ssVVCF formalism from 6.4 ns trajectory (top) and those by using the $\mu\text{-}\alpha$ correlation function from a 9.6 ns MD trajectory (bottom) with various r_t .

function, we simulated the SFG spectra using t ps MD trajectory ($\text{Im}\chi_{aac}^{\text{res},(2)}(\omega; t)$) and calculated the root-mean-square deviation (RMSD) of $\text{Im}\chi_{aac}^{\text{res},(2)}(\omega; t)$ from the fully converged SFG spectrum $\langle \text{Im}\chi_{aac}^{\text{res},(2)}(\omega) \rangle$ as

$$\text{RMSD}(t) = \sqrt{\int_{\omega_1}^{\omega_2} d\omega [\text{Im}\chi_{aac}^{\text{res},(2)}(\omega; t) - \langle \text{Im}\chi_{aac}^{\text{res},(2)}(\omega) \rangle]^2}, \quad (16)$$

where we set $\omega_1 = 3000 \text{ cm}^{-1}$ and $\omega_2 = 3800 \text{ cm}^{-1}$ to cover the whole O–H stretch SFG band. The calculated RMSDs are plotted in Fig. 3, while the corresponding SFG spectra are given in Fig. 4. Figure 3 demonstrates that the response of the O–H stretch SFG spectrum calculated by the ssVVCF

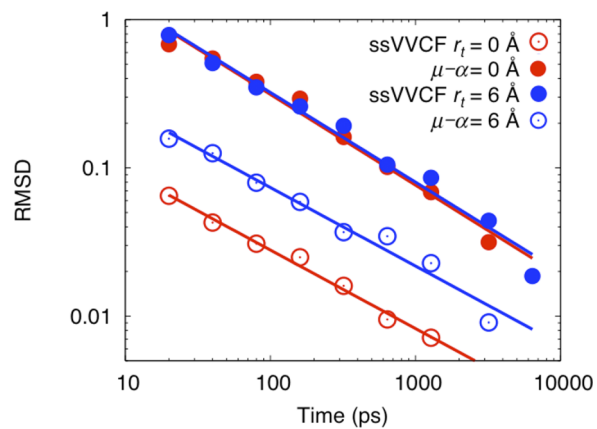


FIG. 3. Root-mean-square deviations (RMSDs) of the error for the SFG spectra calculated with the limited MD trajectories. The lines are fits to the data points to guide the eye.

formalism converges an order of magnitude faster than the $\mu\text{-}\alpha$ time correlation function formalism. When the convergence criterion of RMSD was set to 0.03, only 80 ps MD trajectory is required for computing the SFG spectra via the ssVVCF formalism. Since a 600 ps MD trajectory is needed to achieve the same RMSD criterion for the $\mu\text{-}\alpha$ time correlation function, the ssVVCF is ~ 8 times computationally less expensive than the $\mu\text{-}\alpha$ time correlation function. Note that the 80 ps MD trajectories are in the similar length of the trajectory which is needed for sampling the whole phase space for the molecular conformation of the water-air interface.^{15,71} In contrast to the clear advantage of the ssVVCF algorithm for $r_t = 0 \text{ \AA}$, there is no clear advantage for large cross-correlation cutoff ($r_t = 6 \text{ \AA}$). This indicates that the convergence of the time-correlation function is governed by the cross-correlation terms rather than the fluctuation of the dipole moment and polarizability for larger r_t , and thus the long MD trajectory would be required

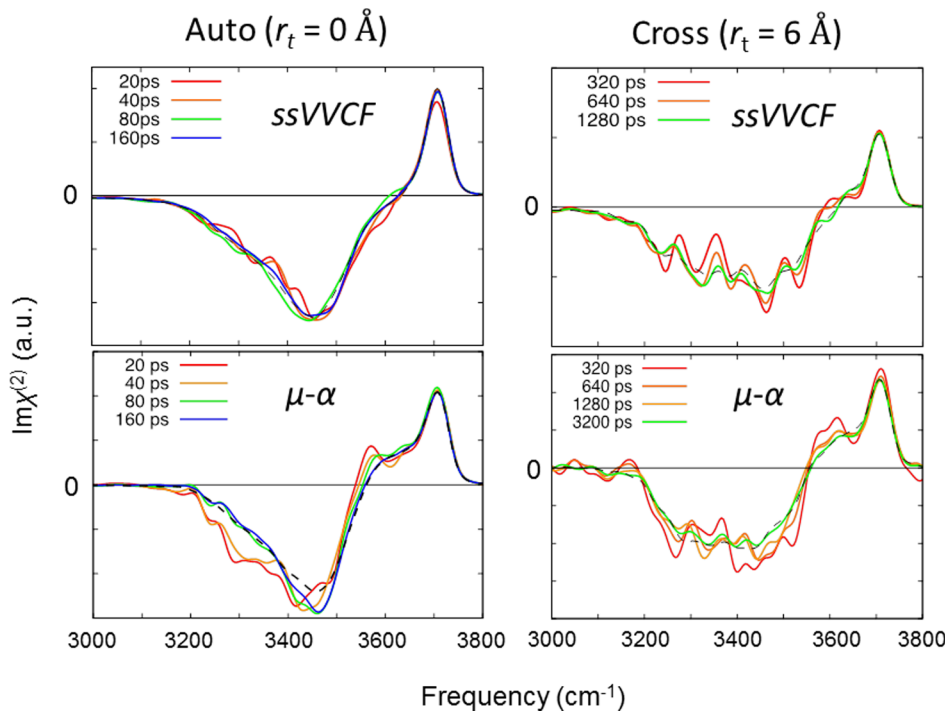


FIG. 4. Simulated O–H stretch SFG spectra with different lengths of trajectories. Spectra calculated from the 6.4 ns and 9.6 ns MD trajectories for ssVVCF and $\mu\text{-}\alpha$ correlation function, respectively, are shown in dashed lines.

for the convergence of both the ssVVCF and the $\mu\text{-}\alpha$ time correlation function. We would like to note that even though the advantage of the ssVVCF formalism disappears for larger r_t , the ssVVCF formalism has still a clear merit that allows us to skip the polarizability calculation with the external electric field.

D. SFG spectra with AIMD trajectories

Having established the accuracy of the ssVVCF formalism for computing the O–H stretch SFG spectra using the force field MD trajectories, we simulated the *ab initio* SFG spectra with different density functionals. Here, we consider only the SFG spectra without any cross-correlation terms, because of the limited (80 ps) AIMD trajectories. Note that since in the $r_t = 0$ Å calculation, all the intra-/inter-molecular couplings are absent, the simulated spectra correspond to the experimentally measured spectra of isotopically diluted water.

The simulated SFG spectra calculated with the PBE, revPBE, and BLYP functionals are displayed in Figure 5. The PBE and revPBE functionals predict a positive free O–H peak at 3740 cm⁻¹, which is 50 cm⁻¹ higher than the peak frequency calculated with the BLYP functional. This trend is the same as the gas-phase calculation for the vibrational mode of a water molecule.¹⁰² Experimentally, the peak frequency of the free O–H stretch mode was 3700 cm⁻¹.²¹ For the negative hydrogen-bonded O–H stretch peak at 3350–3500 cm⁻¹, the PBE functional predicts the lowest O–H stretch frequency for the negative peak, while the revPBE functional predicts the highest frequency. This indicates that the hydrogen bond strength is stronger in the order of PBE > BLYP > revPBE at the water-air interface. This is also consistent with the previous AIMD simulation of the liquid bulk water; the first peak heights in the radial distribution functions of oxygen-oxygen atoms are higher in the order of PBE > BLYP > revPBE.⁹⁷ The use of the BLYP functional reproduces the experimentally measured frequency of the positive free O–H peak and the negative hydrogen-bonded peak^{21,23,103} among several density functionals.

Furthermore, we explored the impact of the van der Waals corrections on the SFG spectra by comparing the SFG spectrum calculated with the BLYP-AIMD trajectories with that with the BLYP + Grimme's D3 van der Waals correction

(BLYP-D)-AIMD trajectories. The BLYP-D-AIMD simulation shows a shallower negative peak than the BLYP-D-AIMD simulation, while the peak frequency is not changed. The smaller peak amplitude of the BLYP-AIMD simulation can be accounted for as follows: The BLYP-AIMD simulation without the van der Waals corrections tends to predict over-structured water.^{97,104} With the overstructured structure of H₂O, the transition dipole moments pointing *up* to the air in the second layer largely cancel out the transition dipole moment pointing *down* to the bulk in the topmost layer. This cancellation leads to the much smaller O–H stretch SFG responses from each O–H stretch chromophore localized on a single water molecule at the overstructured ice-air interface than the SFG response at the water-air interface.¹¹ (Compare SFG spectrum for case 3 ice with the spectrum for liquid water in Fig. 2(b) of Ref. 11.)

In general, water structure in the AIMD simulation with the generalized gradient approximation (GGA) can be improved dramatically by using the dispersion correction.⁹⁷ However, this empirical correction for the dispersion forces is often not sufficient, and thus AIMD-D simulation shows somehow overstructured liquid water. Huge computational cost is needed to simulate the liquid water with higher level of *ab initio* theory. To avoid this drawback and obtain a clear guideline for improving the accuracy of the simulated SFG spectra of the interfacial water, it is important to develop the force fields by fitting the *ab initio* calculated data with the force field models^{105–109} and calculate the SFG spectra with these force field models. It should be also noted that our current simulation does not include the nuclear quantum effects. Nuclear quantum effects alter the inter-/intra-molecular interactions, which are known to affect the vibrational spectra, both through the intensity and the positions of the spectral bands. Specifically, quantum effects have been shown to cause a redshift of the OH-stretch band by ~150–200 cm⁻¹. However, the inclusion of quantum effects in AIMD simulations aimed at calculating the surface vibrational spectra is computationally very demanding and thus it would be a challenge for the next step.¹¹⁰ We note that including quantum effects may lead to shifts and intensity variations of bands, but are not expected to lead to new features in the vibrational response function, such as the positive feature reported in the experimental spectrum at ~3100 cm⁻¹.

Finally, it should be noted that our current results seem to contradict with Ref. 66 where the positive 3100 cm⁻¹ band was present in the SFG spectra calculated from the AIMD trajectories. However, since the spectrum exhibits large fluctuation and the baseline deviates from zero presumably because of the insufficient convergence of the time-correlation function, it would be difficult to conclude that the AIMD simulation performed in Ref. 66 reproduces this positive band. Our study clearly shows that from the well converged time correlation function with the help of the efficient algorithm presented here, the positive band cannot be observed by using the AIMD trajectories.

On the other hand, several force field MD simulations reported the presence of the 3100 cm⁻¹ band using the classical force field model with the three-body interaction potentials. Skinner and co-workers have calculated SFG spectra at the

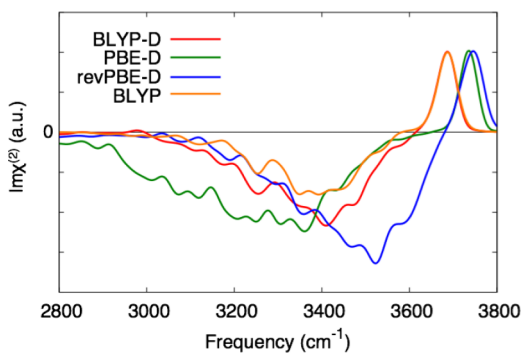


FIG. 5. O–H stretch SFG spectra simulated from the AIMD trajectories at different levels of theory. The spectra are normalized at the dangling O–H peaks centered at ~3700 cm⁻¹.

isotopically diluted water-air interface, showing the positive SFG response around 3100 cm^{-1} with an amplitude similar to that of the negative peak.⁵² On the other hand, Ishiyama and Morita obtained this 3100 cm^{-1} positive peak from their MD simulation by modifying the vibrational response calculation, without including the three-body interactions.²¹ Although both have claimed that the positive 3100 cm^{-1} band is reproduced, the amplitude of this 3100 cm^{-1} positive SFG band in Ref. 21 was fairly weak compared with that in Ref. 51. As such, there remains a qualitative difference between these two different modeling results. This qualitative difference can be also found in experiments. Shen and co-workers have used the picosecond laser pulses and found that the amplitudes of the negative and positive bands of the hydrogen bonded SFG response at the water-air interface are almost identical.²³ This trend is in good agreement with the subsequent measurement performed by Allen and co-workers.³¹ In contrast, Tahara and co-workers and sequentially Bakker and co-workers show relatively weaker positive $\sim 3100\text{ cm}^{-1}$ band with only 30%–40% of the amplitude of the negative bands reported in Refs. 21 and 111. Moreover, very recently, Yamaguchi reported the absence of the 3100 cm^{-1} band at the water-air interface.¹¹² These indicate that beyond the discussion on the presence or absence of the positive 3100 cm^{-1} band, we may need more delicate discussion on this peak such as the amplitude and the zero-crossing point lying between the positive and negative peaks. The fact that the *ab initio* based force field model and the AIMD simulation do not have a 3100 cm^{-1} positive band challenges the force field modeling in the heterogeneous system. Furthermore, beyond the SFG spectrum at room temperature, exploring the effect of temperature variation on the SFG response^{1,5,113} seems to be very helpful to understand the vibrational nature of the O–H stretch vibrational mode at the water-air interface.

V. CONCLUDING REMARKS

We have presented an efficient formalism for computing the SFG spectra of water O–H stretch mode based on the ssVVCF formalism. This algorithm allows us to simulate the SFG spectra at the water-air interface with an order of magnitude shorter MD trajectory compared to the μ - α time correlation function formalism. The calculated SFG spectra with the ssVVCF reproduced well those simulated with the μ - α time correlation function. The recommended MD trajectories for calculating the O–H stretch SFG spectra are 80 ps and 6 ns for the truncating response functions with $r_t = 0\text{ \AA}$ and 6 \AA , respectively.

By employing this formalism, we calculated the SFG spectra at the water-air interface using the AIMD trajectories with various functionals. The comparison of the spectra simulated with the AIMD trajectories with the PBE, BLYP, and revPBE functionals indicates that the weaker and stronger hydrogen bond strength predicted by revPBE and PBE functionals, respectively, provides the blue- and red-shifted negative vibrational spectra not only in the bulk but also at the interface. Moreover, we found that the van der Waals correction does not affect the peak frequency, but it induces the enhancement for the negative 3400 cm^{-1} feature. Comparing

the simulated spectra with the experimental data, the simulation with the BLYP-AIMD trajectories gives the best agreement between simulation and experiment for the SFG spectrum of the O–H stretch mode of interfacial water.

In the current simulation at the water-air interface, we did not observe a positive 3100 cm^{-1} band in the SFG spectra, not only for the *ab initio*-based force field MD simulation, but also for the AIMD simulation. This challenges, again, a complete understanding of the structure and dynamics of the water-air interface from the electronic structure theory^{15,71} and/or the *ab initio*-based force field modeling.^{105–110}

ACKNOWLEDGMENTS

T.O. and T.H. thank to the Grant-in-Aid for Scientific Research on Innovative Area, “The Function of Soft Molecular Systems” from JSPS. Y.N. acknowledges the financial support from the German Science Foundation through the project of No. TRR146. The simulations were performed by using the computational facilities in Institute of Solid State Physics, the University of Tokyo, Institute of Molecular Science, and Rechenzentrum Garching of the Max-Planck Society.

APPENDIX: SEPARATION OF LIBRATIONAL AND VIBRATIONAL DYNAMICS

In this appendix, we show how the rotational dynamics and the intramolecular vibration can be separated for the calculation of the VVCF of the IR response. The time derivative of the molecular dipole moment (Eq. (2)) is given by

$$\dot{\vec{\mu}}_i(t) = \dot{B}_i(t) \left(\vec{\mu}_i^0 + \sum_n \mu'_{i,n} \vec{q}_{i,n}(t) \right) + B_i(t) \left(\sum_n \mu'_{i,n} \dot{\vec{q}}_{i,n}(t) \right). \quad (\text{A1})$$

The correlation function is calculated as

$$\begin{aligned} \langle \dot{\vec{\mu}}_i(0) \dot{\vec{\mu}}_j(t) \rangle &= \vec{\mu}_i^0 \vec{\mu}_j^0 \langle \dot{B}_i(0) \dot{B}_j(t) \rangle \\ &+ \sum_{n,m} \mu'_{i,n} \mu'_{j,m} \langle \dot{\vec{q}}_{i,n}^{\text{lab}}(0) \dot{\vec{q}}_{j,m}^{\text{lab}}(t) \rangle \\ &+ \sum_{n,m} \vec{\mu}_i^0 \mu'_{j,m} \langle \dot{B}_i(0) \dot{\vec{q}}_{j,m}^{\text{lab}}(t) + \dot{\vec{q}}_{i,n}^{\text{lab}}(0) \dot{B}_j(t) \rangle, \end{aligned} \quad (\text{A2})$$

where we used

$$\dot{\vec{q}}_{i,n}^{\text{lab}}(t) = \dot{B}_i(t) \vec{q}_{i,n}(t) + B_i(t) \dot{\vec{q}}_{i,n}(t). \quad (\text{A3})$$

The first term in the right hand side of Eq. (A2) denotes the librational motion, which provides the peaks at the O–H librational mode frequency range (400 – 1000 cm^{-1}). Thus, the first term can be omitted when the O–H stretch mode (3000 – 3600 cm^{-1}) is discussed. Furthermore, it is reasonably assumed that the O–H stretch mode is decoupled from the librational mode as the first approximation since these normal modes are orthogonal to each other. By assuming this, the third term in the right hand side of Eq. (A2) is zero, and the expression reduces to Eq. (5). The same discussion holds for the derivation for the ssVVCF of the SFG response function.

- ¹Q. Du, R. Superfine, E. Freysz, and Y. R. Shen, *Phys. Rev. Lett.* **70**, 2313 (1993).
- ²J. M. Hankett, Y. Liu, X. Zhang, C. Zhang, and Z. Chen, *J. Polym. Sci., Part B: Polym. Phys.* **51**, 311 (2013).
- ³L. F. Scatena, M. G. Brown, and G. L. Richmond, *Science* **292**, 908 (2001).
- ⁴R. Vächa, S. W. Rick, P. Jungwirth, A. G. F. de Beer, H. B. de Aguiar, J.-S. Samson, and S. Roke, *J. Am. Chem. Soc.* **133**, 10204 (2011).
- ⁵S. Strazdaite, J. Versluis, E. H. G. Backus, and H. J. Bakker, *J. Chem. Phys.* **140**, 054711 (2014).
- ⁶K. Meister, S. Strazdaite, A. L. DeVries, S. Lotze, L. L. C. Olijve, I. K. Voets, and H. J. Bakker, *Proc. Natl. Acad. Sci. U. S. A.* **111**, 17732 (2014).
- ⁷S. Ma, H. Li, K. Tian, S. Ye, and Y. Luo, *J. Phys. Chem. Lett.* **5**, 419 (2014).
- ⁸L. Fu, J. Liu, and E. C. Y. Yan, *J. Am. Chem. Soc.* **133**, 8094 (2011).
- ⁹M. Okuno and T.-A. Ishibashi, *J. Phys. Chem. C* **119**, 9947 (2015).
- ¹⁰H. Groenzin, I. Li, V. Buch, and M. J. Shultz, *J. Chem. Phys.* **127**, 214502 (2007).
- ¹¹T. Ishiyama, H. Takahashi, and A. Morita, *J. Phys. Chem. Lett.* **3**, 3001 (2012).
- ¹²X. Wei, P. B. Miranda, and Y. R. Shen, *Phys. Rev. Lett.* **86**, 1554 (2001).
- ¹³S. Gopalakrishnan, P. Jungwirth, D. J. Tobias, and H. C. Allen, *J. Phys. Chem. B* **109**, 8861 (2005).
- ¹⁴C. Schnitzer, S. Baldelli, and M. J. Shultz, *Chem. Phys. Lett.* **313**, 416 (1999).
- ¹⁵I. F. W. Kuo and C. J. Mundy, *Science* **303**, 658 (2004).
- ¹⁶M. J. Shultz, P. Bisson, and V. Tuan Hoang, *Chem. Phys. Lett.* **588**, 1 (2013).
- ¹⁷M. J. Shultz, P. Bisson, and T. H. Vu, *J. Chem. Phys.* **141**, 18C521 (2014).
- ¹⁸C. S. Hsieh, R. K. Campen, A. C. V. Verde, P. Bolhuis, H. K. Nienhuys, and M. Bonn, *Phys. Rev. Lett.* **107**, 116102 (2011).
- ¹⁹J. Liu, R. S. Andino, C. M. Miller, X. Chen, D. M. Wilkins, M. Ceriotti, and D. E. Manolopoulos, *J. Phys. Chem. C* **117**, 2944 (2013).
- ²⁰Y. Nagata, R. E. Pool, E. H. G. Backus, and M. Bonn, *Phys. Rev. Lett.* **109**, 226101 (2012).
- ²¹S. Nihonyanagi, T. Ishiyama, T.-K. Lee, S. Yamaguchi, M. Bonn, A. Morita, and T. Tahara, *J. Am. Chem. Soc.* **133**, 16875 (2011).
- ²²I. V. Stiopkin, C. Weeraman, P. A. Pieniazek, F. Y. Shalhout, J. L. Skinner, and A. V. Benderskii, *Nature* **474**, 192 (2011).
- ²³C.-S. Tian and Y. R. Shen, *J. Am. Chem. Soc.* **131**, 2790 (2009).
- ²⁴Z. Zhang, L. Piatkowski, H. J. Bakker, and M. Bonn, *Nat. Chem.* **3**, 888 (2011).
- ²⁵M. Bonn, Y. Nagata, and E. H. G. Backus, *Angew. Chem., Int. Ed.* **54**, 5560 (2015).
- ²⁶R.-R. Feng, Y. Guo, R. Lü, L. Velarde, and H.-F. Wang, *J. Phys. Chem. A* **115**, 6015 (2011).
- ²⁷C. Y. Wang, H. Groenzin, and M. J. Shultz, *J. Am. Chem. Soc.* **126**, 8094 (2004).
- ²⁸C. S. Tian and Y. R. Shen, *Proc. Natl. Acad. Sci. U. S. A.* **106**, 15148 (2009).
- ²⁹L. Zhang, C. Tian, G. A. Waychunas, and Y. R. Shen, *J. Am. Chem. Soc.* **130**, 7686 (2008).
- ³⁰J. A. McGuire and Y. R. Shen, *Science* **313**, 1945 (2006).
- ³¹X. K. Chen, W. Hua, Z. S. Huang, and H. C. Allen, *J. Am. Chem. Soc.* **132**, 11336 (2010).
- ³²S. Nihonyanagi, J. A. Mondal, S. Yamaguchi, and T. Tahara, *Annu. Rev. Phys. Chem.* **64**, 579 (2013).
- ³³S. Nihonyanagi, S. Yamaguchi, and T. Tahara, *J. Chem. Phys.* **130**, 204704 (2009).
- ³⁴D. Verreault, W. Hua, and H. C. Allen, *J. Phys. Chem. Lett.* **3**, 3012 (2012).
- ³⁵J. F. Davies, R. E. H. Miles, A. E. Haddrell, and J. P. Reid, *Proc. Natl. Acad. Sci. U. S. A.* **110**, 8807 (2013).
- ³⁶D. L. Bones, J. P. Reid, D. M. Lienhard, and U. K. Krieger, *Proc. Natl. Acad. Sci. U. S. A.* **109**, 11613 (2012).
- ³⁷M. Shiraiwa, M. Ammann, T. Koop, and U. Poeschl, *Proc. Natl. Acad. Sci. U. S. A.* **108**, 11003 (2011).
- ³⁸K. Uosaki, T. Yano, and S. Nihonyanagi, *J. Phys. Chem. B* **108**, 19086 (2004).
- ³⁹T. Ishiyama and A. Morita, *J. Phys. Chem. C* **111**, 721 (2007).
- ⁴⁰A. Morita and J. T. Hynes, *Chem. Phys.* **258**, 371 (2000).
- ⁴¹A. Morita and J. T. Hynes, *J. Phys. Chem. B* **106**, 673 (2002).
- ⁴²Y. Nagata and S. Mukamel, *J. Am. Chem. Soc.* **132**, 6434 (2010).
- ⁴³S. Roy and D. K. Hore, *J. Phys. Chem. C* **116**, 22867 (2012).
- ⁴⁴S. A. Hall, K. C. Jena, P. A. Covert, S. Roy, T. G. Trudeau, and D. K. Hore, *J. Phys. Chem. B* **118**, 5617 (2014).
- ⁴⁵H. M. Chase, B. T. Psciuik, B. L. Strick, R. J. Thomson, V. S. Batista, and F. M. Geiger, *J. Phys. Chem. A* **119**, 3407 (2015).
- ⁴⁶B. M. Auer and J. L. Skinner, *J. Chem. Phys.* **129**, 214705 (2008).
- ⁴⁷R. Kumar and J. L. Skinner, *J. Phys. Chem. B* **112**, 8311 (2008).
- ⁴⁸A. Perry, C. Neipert, B. Space, and P. B. Moore, *Chem. Rev.* **106**, 1234 (2006).
- ⁴⁹B. M. Auer and J. L. Skinner, *J. Phys. Chem. B* **113**, 4125 (2009).
- ⁵⁰P. A. Pieniazek, C. J. Tainter, and J. L. Skinner, *J. Chem. Phys.* **135**, 044701 (2011).
- ⁵¹P. A. Pieniazek, C. J. Tainter, and J. L. Skinner, *J. Am. Chem. Soc.* **133**, 10360 (2011).
- ⁵²C. J. Tainter, P. A. Pieniazek, Y.-S. Lin, and J. L. Skinner, *J. Chem. Phys.* **134**, 184501 (2011).
- ⁵³T. Ishiyama and A. Morita, *J. Chem. Phys.* **131**, 244714 (2009).
- ⁵⁴T. Ishiyama, H. Takahashi, and A. Morita, *Phys. Rev. B* **86**, 035408 (2012).
- ⁵⁵T. Ishiyama and A. Morita, *J. Phys. Chem. C* **113**, 16299 (2009).
- ⁵⁶S. J. Byrnes, P. L. Geissler, and Y. R. Shen, *Chem. Phys. Lett.* **516**, 115 (2011).
- ⁵⁷T. Ishiyama, T. Imamura, and A. Morita, *Chem. Rev.* **114**, 8447 (2014).
- ⁵⁸J. Noah-Vanhoucke, J. D. Smith, and P. L. Geissler, *J. Phys. Chem. B* **113**, 4065 (2009).
- ⁵⁹M. D. Baer, I. F. W. Kuo, D. J. Tobias, and C. J. Mundy, *J. Phys. Chem. B* **118**, 8364 (2014).
- ⁶⁰R. Car and M. Parrinello, *Phys. Rev. Lett.* **55**, 2471 (1985).
- ⁶¹T. Frigato, J. VandeVondele, B. Schmidt, C. Schütte, and P. Jungwirth, *J. Phys. Chem. A* **112**, 6125 (2008).
- ⁶²M. P. Gaigeot and M. Sprik, *J. Phys. Chem. B* **107**, 10344 (2003).
- ⁶³M. Heyden, J. Sun, S. Funkner, G. Mathias, H. Forbert, M. Havenith, and D. Marx, *Proc. Natl. Acad. Sci. U. S. A.* **107**, 12068 (2010).
- ⁶⁴H. S. Lee and M. E. Tuckerman, *J. Chem. Phys.* **126**, 164501 (2007).
- ⁶⁵M. Sulpizi, M. Salanne, M. Sprik, and M. P. Gaigeot, *J. Phys. Chem. Lett.* **4**, 83 (2013).
- ⁶⁶J. Sun, D. Bousquet, H. Forbert, and D. Marx, *J. Chem. Phys.* **133**, 114508 (2010).
- ⁶⁷T. D. Kühne and R. Z. Khaliullin, *Nat. Commun.* **4**, 1450 (2013).
- ⁶⁸Y. Nagata, S. Yoshimune, C.-S. Hsieh, J. Hunger, and M. Bonn, *Phys. Rev. X* **5**, 021002 (2015).
- ⁶⁹K. Usui, J. Hunger, M. Sulpizi, T. Ohto, M. Bonn, and Y. Nagata, *J. Phys. Chem. B* **119**, 10597 (2015).
- ⁷⁰J. Jeon, J. H. Lim, S. Kim, H. Kim, and M. Cho, *J. Phys. Chem. A* **119**, 5356 (2015).
- ⁷¹T. D. Kühne, T. A. Pascal, E. Kaxiras, and Y. Jung, *J. Phys. Chem. Lett.* **2**, 105 (2011).
- ⁷²L.-M. Liu, C. Zhang, G. Thornton, and A. Michaelides, *Phys. Rev. B* **82**, 161415 (2010).
- ⁷³M. Sumita, C. Hu, and Y. Tateyama, *J. Phys. Chem. C* **114**, 18529 (2010).
- ⁷⁴F. Paesani, S. S. Xantheas, and G. A. Voth, *J. Phys. Chem. B* **113**, 13118 (2009).
- ⁷⁵H. Nakamura, T. Ohto, and Y. Nagata, *J. Chem. Theory Comput.* **9**, 1193 (2013).
- ⁷⁶T. Ohto, A. Mishra, S. Yoshimune, H. Nakamura, M. Bonn, and Y. Nagata, *J. Phys.: Condens. Matter* **26**, 244102 (2014).
- ⁷⁷J. Cheng and M. Sprik, *J. Chem. Theory Comput.* **6**, 880 (2010).
- ⁷⁸J. Cheng and M. Sprik, *J. Phys.: Condens. Matter* **26**, 244108 (2014).
- ⁷⁹S. Schnur and A. Gross, *New J. Phys.* **11**, 125003 (2009).
- ⁸⁰Y. Nagata, C.-S. Hsieh, T. Hasegawa, J. Völl, E. H. G. Backus, and M. Bonn, *J. Phys. Chem. Lett.* **4**, 1872 (2013).
- ⁸¹S. Mukamel, *Principles of Nonlinear Optical Spectroscopy* (Oxford University, New York, 1995).
- ⁸²J. Liu, W. H. Miller, F. Paesani, W. Zhang, and D. A. Case, *J. Chem. Phys.* **131**, 164509 (2009).
- ⁸³A. G. F. de Beer, J. S. Samson, W. Hua, Z. S. Huang, X. K. Chen, H. C. Allen, and S. Roke, *J. Chem. Phys.* **135**, 224701 (2011).
- ⁸⁴M. Sovago, R. K. Campen, H. J. Bakker, and M. Bonn, *Chem. Phys. Lett.* **470**, 7 (2009).
- ⁸⁵Z. Wang, Y. Pang, and D. D. Dratt, *J. Chem. Phys.* **120**, 8345 (2004).
- ⁸⁶B. M. Auer and J. L. Skinner, *J. Chem. Phys.* **128**, 224511 (2008).
- ⁸⁷S. A. Corcelli and J. L. Skinner, *J. Phys. Chem. A* **109**, 6154 (2005).
- ⁸⁸T. Hasegawa and Y. Tanimura, *J. Phys. Chem. B* **115**, 5545 (2011).
- ⁸⁹G. Bussi, D. Donadio, and M. Parrinello, *J. Chem. Phys.* **126**, 014101 (2007).
- ⁹⁰P. H. Berens and K. R. Wilson, *J. Chem. Phys.* **74**, 4872 (1981).
- ⁹¹A. D. Becke, *Phys. Rev. A* **38**, 3098 (1988).
- ⁹²C. T. Lee, W. T. Yang, and R. G. Parr, *Phys. Rev. B* **37**, 785 (1988).
- ⁹³J. P. Perdew, K. Burke, and M. Ernzerhof, *Phys. Rev. Lett.* **77**, 3865 (1996).
- ⁹⁴Y. Zhang and W. Yang, *Phys. Rev. Lett.* **80**, 890 (1998).
- ⁹⁵S. Goedecker, M. Teter, and J. Hutter, *Phys. Rev. B* **54**, 1703 (1996).

- ⁹⁶R. Jonchiere, A. P. Seitsonen, G. Ferlat, A. M. Saitta, and R. Vuilleumier, *J. Chem. Phys.* **135**, 154503 (2011).
- ⁹⁷I. C. Lin, A. P. Seitsonen, I. Tavernelli, and U. Rothlisberger, *J. Chem. Theory Comput.* **8**, 3902 (2012).
- ⁹⁸I. C. Lin, A. P. Seitsonen, M. D. Coutinho-Neto, I. Tavernelli, and U. Rothlisberger, *J. Phys. Chem. B* **113**, 1127 (2009).
- ⁹⁹S. Grimme, J. Antony, S. Ehrlich, and H. Krieg, *J. Chem. Phys.* **132**, 154104 (2010).
- ¹⁰⁰J. VandeVondele, M. Krack, F. Mohamed, M. Parrinello, T. Chassaing, and J. Hutter, *Comput. Phys. Commun.* **167**, 103 (2005).
- ¹⁰¹See <http://cp2k.berlios.de/> for the CP2K developers group, 2015.
- ¹⁰²A. Buczek, T. Kupka, and M. A. Broda, *J. Mol. Model.* **17**, 2029 (2011).
- ¹⁰³E. A. Raymond, T. L. Tarbuck, M. G. Brown, and G. L. Richmond, *J. Phys. Chem. B* **107**, 546 (2003).
- ¹⁰⁴J. Schmidt, J. VandeVondele, I. F. W. Kuo, D. Sebastiani, J. I. Siepmann, J. Hutter, and C. J. Mundy, *J. Phys. Chem. B* **113**, 11959 (2009).
- ¹⁰⁵D. Alfè, A. P. Bartók, G. Csányi, and M. J. Gillan, *J. Chem. Phys.* **141**, 014104 (2014).
- ¹⁰⁶G. R. Medders, V. Babin, and F. Paesani, *J. Chem. Theory Comput.* **9**, 1103 (2013); **10**, 2906 (2014).
- ¹⁰⁷M. A. Morales, J. R. Gergely, J. McMinis, J. M. McMahon, J. Kim, and D. M. Ceperley, *J. Chem. Theory Comput.* **10**, 2355 (2014).
- ¹⁰⁸S. Fritsch, R. Potestio, D. Donadio, and K. Kremer, *J. Chem. Theory Comput.* **10**, 816 (2014).
- ¹⁰⁹G. R. Medders and F. Paesani, *J. Chem. Theory Comput.* **11**, 1145 (2015).
- ¹¹⁰J. Kessler, H. Elgabarty, T. Spura, K. Karhan, P. Partovi-Azar, A. A. Hassanali, and T. D. Kühne, *J. Phys. Chem. B* **119**, 10079 (2015).
- ¹¹¹S. Strazdaite, J. Versluis, and H. J. Bakker, *J. Chem. Phys.* **143**, 084708 (2015).
- ¹¹²S. Yamaguchi, *J. Chem. Phys.* **143**, 034202 (2015).
- ¹¹³Y. Nagata, T. Hasegawa, E. H. G. Backus, K. Usui, S. Yoshimune, T. Ohto, and M. Bonn, *Phys. Chem. Chem. Phys.* **17**, 23559 (2015).